BIOLOGY OF REPRODUCTION **82,** 1227–1236 (2010)
Published online before print 24 February 2010.
DOI 10.1095/biolreprod.109.079202

EPAS1 Is Required for Spermatogenesis in the Postnatal Mouse Testis[1]

Michaela Gruber,[3,4] Lijoy K. Mathew,[3,5] Anja C. Runge,[5] Joseph A. Garcia,[6] and M. Celeste Simon[2,4,5]

Abramson Family Cancer Research Institute,[4] University of Pennsylvania School of Medicine, Philadelphia, Pennsylvania
Howard Hughes Medical Institute,[5] University of Pennsylvania, Philadelphia, Pennsylvania
Department of Internal Medicine,[6] University of Texas Southwestern Medical Center at Dallas, Dallas, Texas

ABSTRACT

Spermatogenesis, a process involving the differentiation of spermatogonial stem cells into mature spermatozoa, takes place throughout masculine life. A complex system in the testis, including endocrine signaling, physical interactions between germ and somatic cells, spermatocyte meiosis, and timely release of spermatozoa, controls this cycle. We demonstrate herein that decreased O_2 levels and *Epas1* activation are critical components of spermatogenesis. Postnatal *Epas1* ablation leads to male infertility, with reduced testis size and weight. While immature spermatogonia and spermatocytes are present in *Epas1*$^{Delta/Delta}$ testes, spermatid and spermatozoan numbers are dramatically reduced. This is not due to germ cell-intrinsic defects. Rather, *Epas*$^{Delta/Delta}$ Sertoli cells exhibit decreased ability to form tight junctions, thereby disrupting the blood-testis barrier necessary for proper spermatogenesis. Reduced numbers of tight junction complexes are due to decreased expression of multiple genes encoding tight junction proteins, including TJP1 (ZO1), TJP2 (ZO2), and occludin. Furthermore, *Epas1*$^{Delta/Delta}$ testes exhibit disrupted basement membranes surrounding the seminiferous tubules, causing the premature release of incompletely differentiated germ cells. We conclude that low O_2 levels in the male gonad regulate germ cell homeostasis in this organ via EPAS1.

developmental biology, hypoxia, Sertoli cells, signal transduction, sperm, spermatogenesis, testis, tight junctions

INTRODUCTION

Mammalian spermatogenesis is a complex process involving precisely regulated stem cells, coordinated hormone and growth factor signaling, and a maturation and release process that ensures sperm production throughout masculine life. Germ cells are specified and separated from somatic cells during early embryogenesis. As the embryonic testes are formed, Sertoli cells sequester gonocytes inside the newly formed seminiferous tubules (testicular cords), preventing them from entering meiosis. After birth, Sertoli cells and germ cells undergo rapid proliferation. Tight junctions are formed between Sertoli cells from 7 to 14 days postpartum (dpp) to create the blood-testis barrier (BTB), and germ cells enter meiosis and differentiate into spermatozoa [1]. The Sertoli cells, which are directly attached to the basement membrane, are also connected to the spermatogonia and provide nutrients and regulatory factors. Tight junction complexes are formed between adjacent Sertoli cells, thereby creating an outer (basal) and inner or adluminal compartment. Disruption of these junctions results in defects in spermatogenesis. Serum macromolecules are effectively excluded from the adluminal section, which is an essential prerequisite for spermatogenesis, creating a microenvironment consisting exclusively of Sertoli cell secretions and germ cells [2–4].

Also attached to the basement membrane are the most undifferentiated germ cells, the type A spermatogonia (see Figs. 4A and 9C). Spermatogonial stem cells (SSCs), like other stem cells in the organism, are characterized by their ability to self-renew and maintain an appropriate number of undifferentiated cells. As these cells differentiate, they migrate away from the lamina and toward the tubular lumen, where they are released upon maturation into spermatozoa. The systematic maintenance of spermatogenesis is controlled by a number of factors, including hormones, temperature, and O_2 availability. Evidence shows that the testis is hypoxic and that the spatially well-orchestrated process of spermatogenesis occurs along a profound O_2 partial pressure gradient [5].

The ability to control O_2 homeostasis is essential for multicellular organisms. The cardiovascular, hematopoietic, and respiratory organs provide proper oxygenation to all cells and tissues. Whereas ambient air contains 21% O_2, most tissues maintain O_2 tensions between 2% and 9%. Of note, the testis has been reported to be a naturally O_2-deprived organ [5]. Decreased O_2, or ''hypoxia,'' occurs in a number of processes (e.g., embryonic development, postnatal organogenesis, and disease). The heterodimeric hypoxia-inducible factors (HIFs) are critical transcriptional regulators of systemic and cellular responses to hypoxia [6–8]. HIFs consist of an α subunit (usually HIF-1α or EPAS1) and a β subunit (HIF-β, also known as ARNT for aryl hydrocarbon receptor nuclear translocator). HIF activity is regulated via the labile α subunit [9–11], whereas ARNT is expressed constitutively in the nucleus. Upon α subunit stabilization, HIF-α-ARNT dimers bind to hypoxia-response elements to stimulate target genes regulating erythropoiesis, cell survival, metabolism, and vascular remodeling [12]. Despite extensive amino acid sequence homology, HIF1A and EPAS1 (also known as HIF-2α) exhibit different expression patterns and regulate common and unique target genes [13]. In humans, a testis-specific dominant negative isoform of HIF1A is expressed, suggesting a complex functional role for this protein during spermatogenesis [14]. Furthermore, application of unilateral testicular ischemia in rats induces HIF1A at the protein level, indicating HIFs may mediate cellular responses to ischemic stress in this organ [15]. Lysiak et al. [16] demonstrated that murine HIF1A can be detected in interstitial Leydig cells and regulates the promoter of 3β-hydroxysteroid dehydrogenase type 1 (a key

[1]Supported by National Institutes of Health grant 66310 and the Abramson Family Cancer Research Institute. M.C.S. is an investigator for the Howard Hughes Medical Institute.
[2]Correspondence: M. Celeste Simon, Abramson Family Cancer Research Institute, University of Pennsylvania School of Medicine, Philadelphia, PA 19104. FAX: 215 746 5511;
e-mail: celeste2@mail.med.upenn.edu
[3]These authors contributed equally to this work.

Received: 1 June 2009.
First decision: 1 July 2009.
Accepted: 18 February 2010.

eISSN: 1529-7268 http://www.biolreprod.org
ISSN: 0006-3363

enzyme in testosterone production) in vitro. Multiple studies [14–17] suggest that HIF1A has a role in the male reproductive system; however, no in vivo analyses have confirmed that this is the case. Furthermore, the functional role of EPAS1 in testes has not yet been determined.

While *Hif1a*-, *Epas1*-, and *Arnt*-null mice are embryonic lethal [18–23], conditional alleles have allowed the investigation of HIF activity in adult animals [22, 24–28]. We have created a conditional *Epas1* allele and acutely ablated this α subunit after birth. $Epas1^{\Delta/\Delta}$ mice exhibit anemia due to insufficient expression of the EPAS1-specific target gene erythropoietin (*Epo*) [25]. In the present study, we focused on a novel developmental process dependent on EPAS1 spermatogenesis. We deleted *Epas1* within the first week after birth and examined the resulting disruption of spermatid production in normal conditions. Postpubertal $Epas1^{\Delta/\Delta}$ testes exhibited substantially reduced numbers of spermatids but contained spermatogonia, spermatocytes, and Sertoli cells within the seminiferous tubules. This phenotype was not due to germ cell-intrinsic defects but rather cell nonautonomous regulation of spermatogenesis via *Epas1* expression in Sertoli cells. Furthermore, the phenotype progressed with age; $Epas1^{\Delta/\Delta}$ testes became fibrotic, and the basement membrane establishing the seminiferous tubules disintegrated at age 4 mo, resulting in increased germ cell depletion. Of note, $Hif1a^{\Delta/\Delta}$ mice displayed normal testes. Immunohistochemical marker analysis of the basement membrane and myoid cell layers, as well as functional BTB assays, revealed compromised integrity of these structures. We concluded that EPAS1 (and not HIF1A) regulates the expression of genes encoding Sertoli cell tight junction proteins (e.g., TJP1 and TJP2 [hereafter referred to as ZO1 and ZO2] and occludin) that establish an effective BTB.

MATERIALS AND METHODS

Mouse Experiments

The conditional allele of the murine *Epas1* locus was generated by flanking exon 2 (encoding the DNA-binding domain) by loxP sites [25]. Mice homozygous for the 2-loxP allele are phenotypically normal and produce wild-type *Epas1* mRNA. Cre-mediated recombination between the loxP sites in the 2-loxP allele produces the 1-loxP allele, which lacks exon 2 and produces a mutant mRNA transcript [25]. $Epas1^{fl/fl}$ females were bred to $Epas1^{fl/\Delta}$ Ubc-Cre heterozygous males, resulting in $Epas1^{fl/\Delta}$ Ubc-Cre^{-} and $Epas1^{fl/\Delta}$ Ubc-Cre^{+} pups. The UBC-Cre transgene encodes a tamoxifen-regulated recombinase, allowing acute deletion of ''floxed'' *Epas1* [29]. *Epas1* was deleted 2 days after birth by administering tamoxifen to the nursing mother, leading to efficient recombination of the *Epas1* locus detected by PCR genotyping at weaning as described previously [25]. All procedures involving mice were performed in accord with National Institutes of Health (Bethesda, MD) guidelines for use and care of live animals and were approved by the University of Pennsylvania Institutional Animal Care and Use Committee.

Histology, Immunohistochemistry, and Immunofluorescence

Testes from mice at ages 2, 4, 7, and 13 mo (see *Results*) were harvested in PBS, fixed in 4% paraformaldehyde at 4°C for 24 h, dehydrated through an inclining EtOH series into 100% EtOH, treated with xylene, and embedded in paraffin (n = 3–5). Whole-body perfusion was also used as an alternative tissue fixation process. Briefly, the mice were anesthetized, and warm PBS was infused through the right ventricle, while the right auricle was punctured with scissors, allowing the fluids to exit. This was followed by perfusion with 2% glutaraldehyde using a similar method, and testes were harvested. The testes were then transferred to osmium tetroxide, embedded in epon, and 1-μm-thin sections were used for toludine blue staining for histological analysis. Hematoxylin-eosin (H&E) staining was performed by standard protocols [25]. Immunohistochemistry (IHC) and immunofluorescence (IF) were performed on 5-μm sections based on standard procedures. The antibodies used were goat GATA4 (C-20) (1:150) and rabbit ZO-2 (1:50) (both from Santa Cruz Biotechnology, Santa Cruz, CA); rabbit POU5F1 (1:150), rabbit VASA (1:750), mouse PCNA1 (1:1000), rabbit SCP3 (1:300), rabbit SMA (prediluted), and rabbit ZO-1 (1:100) (all from Abcam, Cambridge, MA); rabbit cleaved caspase 3 (1:200) and rabbit p-H2AX (1:300) (both from Cell Signaling, Danvers, MA); and rabbit collagen IV (1:50) (Millipore, Billerica, MA). The FE-J1 antibody (1:200), developed by Bruce Fenderson, was obtained from the Developmental Studies Hybridoma Bank developed under the auspices of the Eunice Kennedy Shriver National Institute of Child Health and Human Development (Rockville, MD) and maintained by the Department of Biological Sciences, University of Iowa, Iowa City, IA. Also used were secondary antibodies to goat (avidin-biotin-peroxidase kit; Vector Labs, Burlingame, CA), rabbit (horseradish peroxidase [HRP] conjugated, 1:300; Cell Signaling), fluorescein isothiocyanate (FITC) conjugated (1:500; Sigma, St. Louis, MO) or Texas Red conjugated (1:500; eBioscience, San Diego, CA), and mouse (HRP conjugated, 1:300; Cell Signaling). The thickness of basement membranes was measured using the line segment tool of Adobe Illustrator (Adobe Systems, Mountain View, CA).

Pimonidazole staining was performed using a kit from Chemicon (Billerica, MA) according to the manufacturer's protocol. Briefly, mice were injected with pimonidazole i.p. at a dose of 60 mg/kg on the day of killing, and tissue samples were isolated 1 h later. An HT15 trichrome stain (Masson) kit from Sigma was used according to the manufacturer's manual.

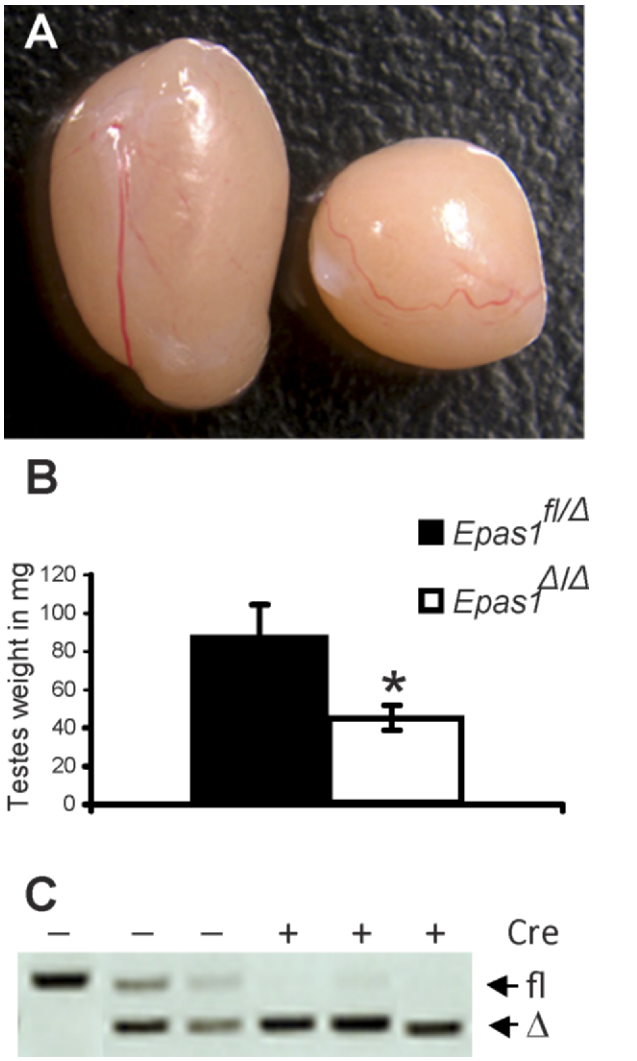

FIG. 1. $Epas1^{\Delta/\Delta}$ testes are reduced in size and weight. **A**) The control testis ($Epas1^{fl/\Delta}$) on the left was approximately twice the size of the $Epas1^{\Delta/\Delta}$ on the right at age 8 wk. Well-defined vasculature was visible at the testis surface of either genotype. Original magnification ×3. **B**) Control testes weighed approximately 80 mg in a 30-g mouse. In contrast, $Epas1^{\Delta/\Delta}$ testes weighed 40 mg each in males displaying the same body weight (n = 5, $^{*}P < 0.05$). **C**) Efficient *Epas1* deletion was confirmed by PCR for the floxed and deleted allele of DNA isolated from control and $Epas1^{\Delta/\Delta}$ testes as previously described [25].

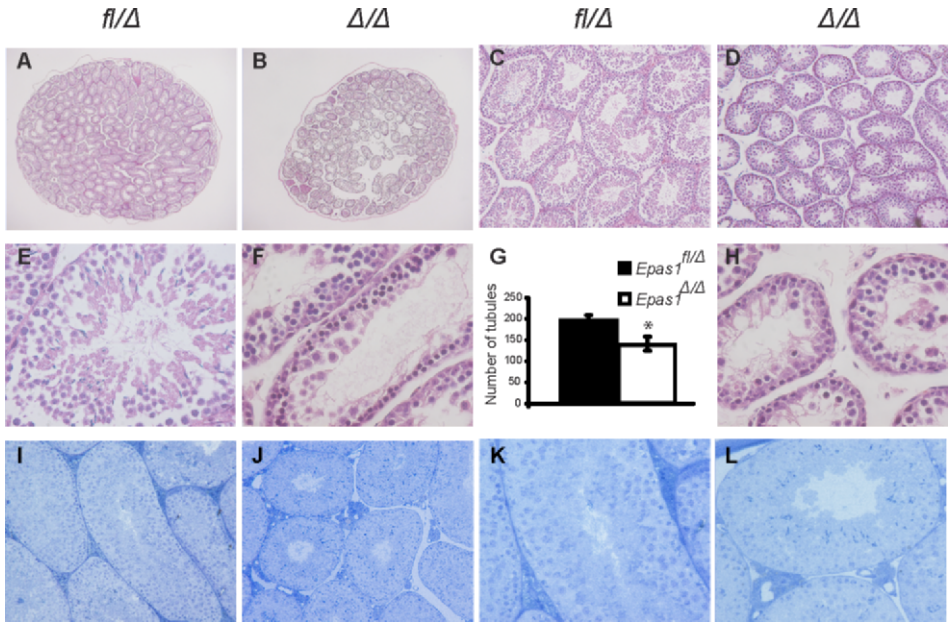

FIG. 2. Loss of *Epas1* resulted in fewer and smaller seminiferous tubules. **A** and **B**) Cross-sections through the center of control and $Epas1^{\Delta/\Delta}$ testes are displayed. The average number of tubules was enumerated and found to be reduced by 25% in $Epas1^{\Delta/\Delta}$ testes (n = 5, $^*P < 0.05$) (**G**). **C** and **D**) $Epas1^{\Delta/\Delta}$ seminiferous tubules have a smaller diameter compared with control testes. **E**, **F**, and **H**) Higher magnification of H&E-stained tissue shows the presence of spermatogonia, spermatocytes, spermatids, and Sertoli cells in control samples but revealed decreased numbers of spermatids in $Epas1^{\Delta/\Delta}$ testes. Cross-sections of control (**I** and **K**) and $Epas1^{\Delta/\Delta}$ (**J** and **L**) testes after fixation by whole-body perfusion and staining with toluidine blue also demonstrated the smaller size of mutant tubules. Original magnification ×20 (**A** and **B**), ×100 (**C** and **D**), × 200 (**I** and **J**), and ×400 (**E**, **F**, **H**, **K**, and **L**).

Quantification of Sertoli, POU5F1$^+$, and Proliferating Cells

The cells were enumerated by manual counting after staining with GATA4, POU5F1, and PCNA antibodies for Sertoli, POU5F1$^+$ spermatogonial, and proliferating cells, respectively. All quantitative measurements of cell numbers are referred to as the number of cells per tubule cross-section. Sertoli cell nuclear area was measured using ImageJ software (National Institutes of Health).

Blood-Testis Barrier Integrity Assay

Integrity of the BTB was analyzed by assessing the ability of the BTB to restrict the diffusion of a small fluorescent probe across the barrier. Briefly, 0.3 mg of FITC (M_r 389; AnaSpec, San Jose, CA) reconstituted in dimethyl sulfate was diluted in sterile saline and administered to $Epas1^{fl/\Delta}$ control or $Epas1^{\Delta/\Delta}$ mice via tail vein injection. The animals were allowed to recover, approximately 30 min later they were killed, and testes were removed and frozen in liquid nitrogen. Frozen testes sections were obtained and examined by fluorescence microscopy.

RNA Analysis

RNA was isolated from whole testis using Trizol (Invitrogen, Carlsbad, CA) according to the manufacturer's manual. Three to five micrograms of RNA was translated to cDNA using oligo-dT and 18S reverse primers and SuperScript RT II (Invitrogen, Carlsbad, CA). Calmegin, MYBL1, and GPD were amplified using primers previously described [30]. Quantitative RT-PCR was performed with gene expression assays from Applied Biosystems (Foster City, CA) for ZO1, ZO2, occludin, transferrin, SMN1, TIMP1, and 18S ribosomal RNA (n = 3).

Serum Testosterone

Testosterone levels in the serum were measured. This was performed by A.F. Parlow at the Harbor-UCLA Research and Education Institute (West Carson, CA).

Statistical Analysis

Statistical analysis was performed using unpaired Student *t*-test. $P < 0.05$ was considered statistically significant, and error bars represent the SEM.

RESULTS

Epas1$^{\Delta/\Delta}$ *Testes Are Reduced in Size and Weight*

Mice harboring a conditional *Epas1* allele were crossed to ubiquitously expressed tamoxifen-inducible Cre-recombinase (UBC-Cre) transgenic mice [29]. By administering tamoxifen to nursing females 2 days after delivery, *Epas1* was uniformly deleted in all tissues of pups positive for Cre-recombinase expression [25]. In addition to the previously reported anemia observed in *Epas1*-deficient mice, these animals were also sterile. Mating $Epas1^{\Delta/\Delta}$ males to wild-type females over a period of 2–3 mo failed to produce any offspring (data not shown). To define mechanisms causing infertility, control and $Epas1^{\Delta/\Delta}$ testes were harvested once puberty was completed (age 6–8 wk). $Epas1^{\Delta/\Delta}$ testes were reduced in size and weight by 50% compared with littermate control males (n = 5, $^*P <$

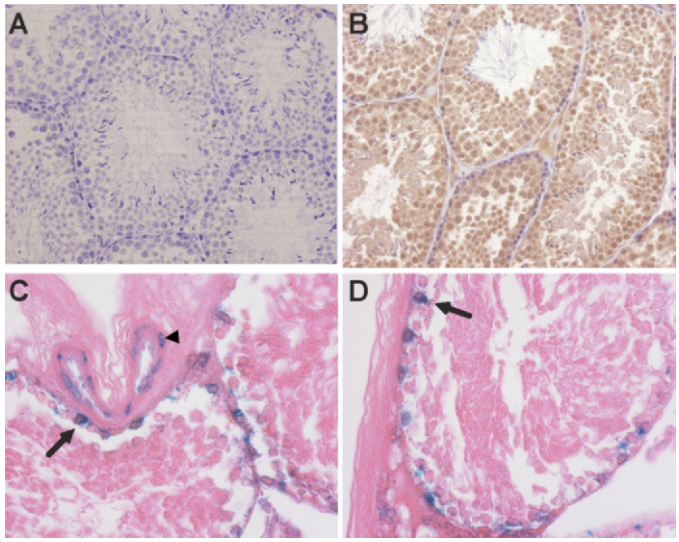

FIG. 3. The testis is a naturally "hypoxic" tissue as determined by pimonidazole staining. Protein thiol adducts recognized by immunohistochemical staining occur in cells experiencing less than 1.5% O_2. **B**) Almost all germ cells exhibited positive staining, confirming low O_2 levels, whereas no staining was observed in testis of animals not injected with pimonidazole (**A**). **C** and **D**) β-Galactosidase activity detected in frozen sections from heterozygous *Epas1:LacZ* knockin testes demonstrates *Epas1* expression in the nuclei of Sertoli cells (arrows) and blood vessel ECs (arrowhead) but not in germ cells. Original magnification ×200 (**A** and **B**) and ×400 (**C** and **D**).

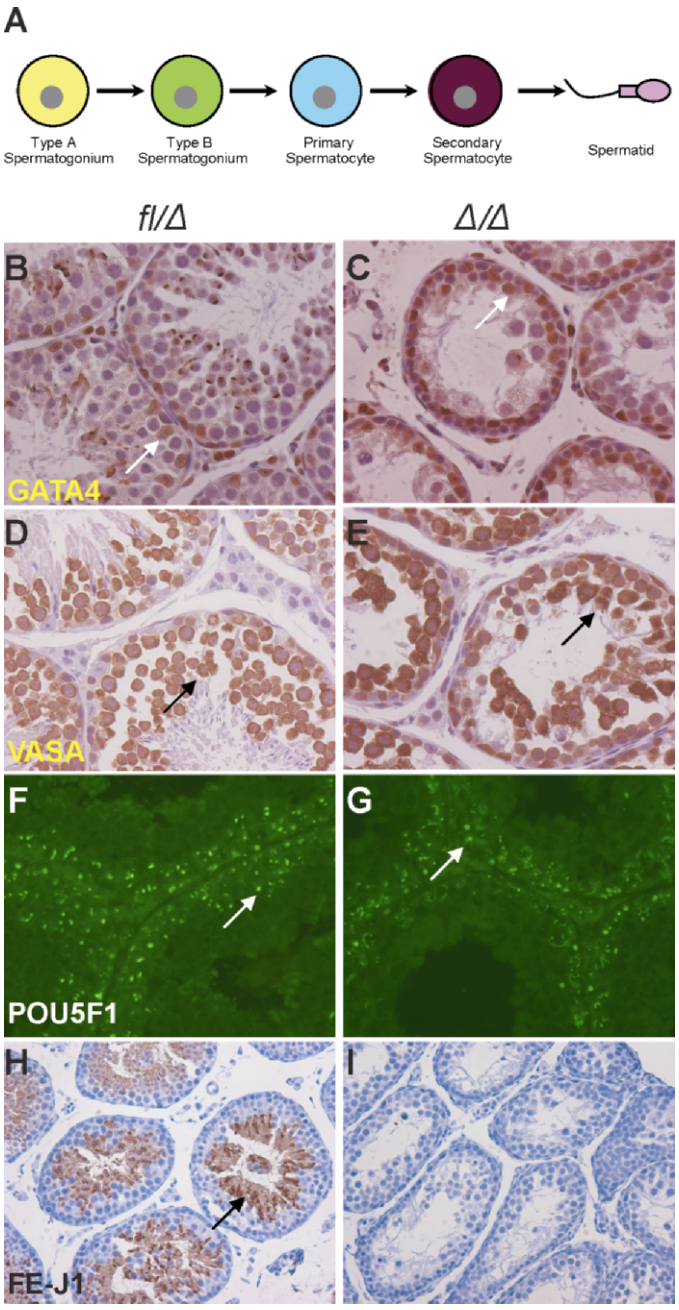

FIG. 4. *Epas1*$^{\Delta/\Delta}$ testes exhibit decreased production of spermatids. **A**) Schematic diagram depicting discrete spermatogenesis. Mitotic divisions of type A and B spermatogonia lead to formation of spermatocytes, followed by meiotic divisions to form spermatids. **B**) GATA4 expression revealed the localization of Sertoli cells attached to the basement membrane and interspersed with germ cells in controls (arrow). **C**) Similar Sertoli cell numbers and position were observed in *Epas1*$^{\Delta/\Delta}$ animals (n = 3–5) (arrow). **D** and **E**) VASA, a cytoplasmic protein expressed in germ cells, confirmed the presence of several layers of germ cells in *Epas1*$^{fl/\Delta}$ and *Epas1*$^{\Delta/\Delta}$ testes (arrows). **E**) Of note, *Epas1*$^{\Delta/\Delta}$ germ cells displayed a disorganized architecture relative to controls. To better assess germ cell types present after *Epas1* ablation, sections were stained for POU5F1 protein expressed in spermatogonia. **F** and **G**) Both control and *Epas1*$^{\Delta/\Delta}$ mice harbored equal numbers of POU5F1^{+} spermatogonia (arrows). **H** and **I**) Haploid spermatids were detected by FE-J1 (a component of the acrosomal complex), staining in control testes (arrow). However, *Epas1*$^{\Delta/\Delta}$ testes were largely devoid of FE-J1-expressing spermatids. Original magnification ×200 (**B**–**E**), ×400 (**F** and **G**), and ×100 (**H** and **I**).

0.05) (Fig. 1, A and B). Blood vessels leading to the testes and the vasculature beneath the testicular capsule appeared normal (Fig. 1A). Efficient *Epas1* deletion within the testis was confirmed by PCR genotyping of testicular DNA (Fig. 1C).

Reduction of Spermatids and Seminiferous Tubule Numbers upon EPAS1 Deletion

Histological analysis of cross-sections through control (*Epas1*$^{fl/\Delta}$) and *Epas1*$^{\Delta/\Delta}$ samples (n = 5, $*P < 0.05$) revealed a 25% reduction in seminiferous tubule numbers (Fig. 2, A and B) in *Epas1*$^{\Delta/\Delta}$ testes (quantified as the number of tubules per testis in Fig. 2G). In addition, the diameter of *Epas1*$^{\Delta/\Delta}$ seminiferous tubules was significantly decreased compared with controls (Fig. 2, C and D). Higher magnification of H&E-stained tissue sections revealed proper architecture and arrangement of Sertoli cells and germ cells at various differentiation stages in control testes (Fig. 2E). Sertoli cells, spermatogonia, and spermatocytes, determined by morphological criteria, were present in their appropriate location in *Epas1*$^{fl/\Delta}$ samples. *Epas1*$^{\Delta/\Delta}$ testes, however, exhibited reduced numbers of round and elongated spermatids and spermatozoa (Fig. 2, F and H). Whole-body perfusion fixation and toludine blue staining revealed a similar phenotype in 2-mo-old mice (i.e., an impaired testicular architecture in *Epas1*-deficient mice (Fig. 2, I–L). However, the reduction in spermatids was not as dramatic in these samples. It is important to note that variations in phenotype were observed in mutant testes due to multiple reasons. Cre-mediated recombination is not always 100% efficient, leading to a slight variability in the extent of phenotypes from mouse to mouse and tubule to tubule. Because the phenotype progresses with age (discussed herein), young mice tend to have a less severe phenotype than older animals. Finally, variation in germ cell loss might be expected from disruption of proper Sertoli cell support of germ cell differentiation (discussed herein). However, it is noteworthy that this phenotype was unique to the EPAS1 isoform, as *Hif1a* [31] deletion using the same system did not affect spermatogenesis (Supplemental Fig. S1, A and A′, available at www.biolreprod.org). In contrast, deficiency in *Arnt*, encoding the EPAS1 heterodimerization partner, phenocopied the lack of spermatids observed in *Epas1*$^{\Delta/\Delta}$ testis (Supplemental Fig. S1, B and B′). These data clearly demonstrate that EPAS1-ARNT dimers are critical for spermatogenesis.

Hypoxia and Epas1 *Expression in the Testis*

To further analyze how EPAS1 regulates germ cell maturation, pimonidazole staining was used to investigate typical O_2 levels of wild-type testes. Pimonidazole forms protein thiol adducts in cells experiencing O_2 concentrations below 1.5% [32]. Figure 3B shows positive staining of essentially all cells within the seminiferous tubules, with relatively rare unstained cells in the interstitial space (n = 3). *Epas1* expression was assessed using previously described *Epas1:LacZ* (encoding β-galactosidase) knockin mice [23]. Frozen sections obtained from testes of heterozygous *Epas1* males displayed β-galactosidase activity and served as a surrogate marker for *Epas1* mRNA expression. Of note, β-galactosidase expression was restricted to the nuclei of Sertoli cells attached to the basement membrane and endothelial cells (ECs) forming blood vessels (Fig. 3, C and D). Double-immunofluorescence for GATA4 (a Sertoli cell marker) and EPAS1 confirmed a Sertoli cell-specific expression pattern within the seminiferous tubule (data not shown).

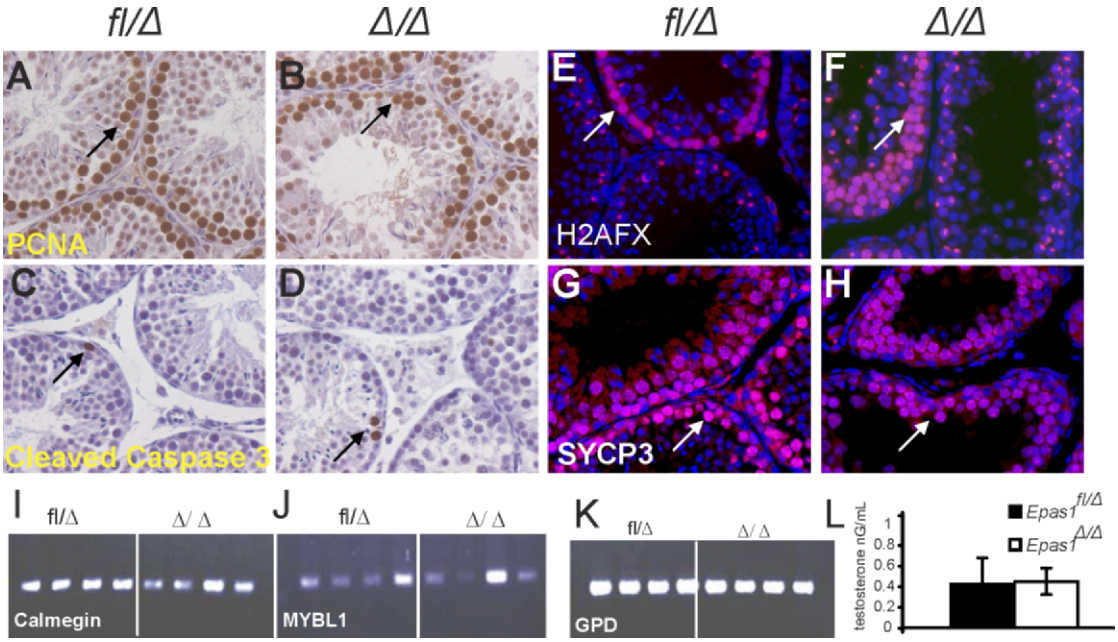

FIG. 5. Proliferation, apoptosis, meiosis, and testosterone levels are not altered in *Epas1*$^{\Delta/\Delta}$ testes. **A** and **B**) Proliferation was not reduced in response to *Epas1* deficiency as assessed by IHC for PCNA1 (n = 4) (arrows). **C** and **D**) Cleaved caspase-3 was used as a means to visualize apoptotic cells. *Epas1*$^{\Delta/\Delta}$ testes did not show increased numbers of dead cells compared with the control testes (arrows). γ-H2AX staining detects double-strand breaks during crossover and remains present in the XY body. **E** and **F**) *Epas1*$^{fl/\Delta}$ and *Epas1*$^{\Delta/\Delta}$ testes displayed a similar staining pattern (arrows). SCP-3 expression connecting the two sister chromatids was used as a second marker for meiosis. **G** and **H**) Testes of both genotypes contained multiple layers of spermatocytes undergoing meiosis (n = 4) (arrows). **I**–**K**) The RT-PCR analysis for calmegin (*Clgn*), *Mybl1*, and *Gpd* (used as a loading control) revealed normal expression of these mRNAs. **L**) Testosterone levels were not changed in *Epas1*-deficient males. Original magnification ×400 (**A**–**H**).

Reduction of Postmeiotic Germ Cells in Epas1$^{\Delta/\Delta}$ *Testes*

During spermatogenesis, spermatogonia divide by mitosis to produce the type A, intermediate, and type B spermatogonium. Type B spermatogonia give rise to primary spermatocytes, followed by secondary spermatocytes, and then mature spermatids (Fig. 4A). The transcription factor GATA4 was used to identify Sertoli cells by IHC [33]. These cells were attached to the basement membrane and interspersed with spermatogonia in control tissues (Fig. 4B). GATA4^{+} cells were localized appropriately in *Epas1*$^{\Delta/\Delta}$ testes, and the number of Sertoli cells per tubule was similar to that in controls (n = 3–5, 27.2 ± 7.9 GATA4^{+} Sertoli cells per tubule in *Epas1*$^{fl/\Delta}$ mice and 29.1 ± 9.8 GATA4^{+} Sertoli cells per tubule in *Epas1*$^{\Delta/\Delta}$ mice) (Fig. 4C). We also measured Sertoli cell nuclear areas (n = 3, 189.93 ± 7.49 arbitrary units in *Epas1*$^{fl/\Delta}$ mice and 172.59 ± 8.53 arbitrary units in *Epas1*$^{\Delta/\Delta}$ mice, $P \leq 0.20$) and did not observe any significant difference in loss of EPAS1 expression. In order to fully characterize the phenotype of *Epas1*$^{\Delta/\Delta}$ testes, we investigated the presence or absence of various cell types within seminiferous tubules after *Epas1* deletion. Morphological analysis of H&E-stained tissue sections suggested germ cell loss after the spermatocyte stage. We performed IHC for VASA, a protein expressed in the cytoplasm of all germ cells, to confirm the presence and localization of germ cells in *Epas1*$^{\Delta/\Delta}$ testes. Whereas several layers of germ cells were present in control testes (Fig. 4D), *Epas1*$^{\Delta/\Delta}$ testes showed disorganized localization and approximately 30%–40% reduction in germ cell number (Fig. 4E). Immunofluorescence staining for POU5F1 (also known as OCT4), a transcription factor expressed in spermatogonia [34], was performed to identify this cell type. Figure 4, F and G, shows POU5F1^{+} type A and type B spermatogonia as one-cell or two-cell layers (with punctate nuclear POU5F1 staining) next to the basement membrane in normal testes. Of note, the punctate nuclear POU5F1 staining was not present in *Pou5f1*$^{\Delta/\Delta}$ testes (Gruber et al., unpublished results), confirming the specificity of the POU5F1 antibody. *Epas1*$^{\Delta/\Delta}$ testes exhibited a POU5F1 expression pattern equivalent to that of littermate controls (Fig. 4, F and G). The number of POU5F1^{+} spermatogonial cells was analyzed, demonstrating no difference in the number per tubule cross-section. Additionally, *Pou5f1* mRNA levels (data not shown) were not altered in *Epas1*$^{\Delta/\Delta}$ specimens, suggesting a defect downstream of the spermatogonial stage. Acrosomal protein FE-J1 staining was used to detect round and elongated spermatids. FE-J1 antibody binds to carbohydrate antigens on the surface of pachytene spermatocytes and spermatids [35]. Multiple layers of FE-J1^{+} germ cells were detected toward the center of the seminiferous tubules in control testes. In direct contrast, *Epas1*$^{\Delta/\Delta}$ testes contained extremely few or no spermatids expressing FE-J1 (Fig. 4, H and I). We concluded that *Epas1* ablation did not affect the SSC pool or immature germ cells but had a severe effect on spermatid and spermatozoa numbers. *Epas1*$^{\Delta/\Delta}$ testes displayed a significant decrease in FE-J1-expressing haploid spermatids. This was further confirmed by microarray analysis, indicating a reduction in mRNAs typically expressed in these cells such as protamine 3 (*Prm3*), transition protein 1 (*Tnp1*), and spermatid-associated protein (*Spert*) (data not shown).

Reduced Numbers of Differentiated Germ Cells in Epas1$^{\Delta/\Delta}$ *Testes Are Not Due to Altered Proliferation, Apoptosis, Meiosis, or Testosterone Levels*

A reduced number of germ cells could be caused by decreased cell proliferation or increased apoptosis in *Epas1*$^{\Delta/\Delta}$ testes. We investigated this possibility by performing IHC for PCNA1, allowing the detection of proliferating cells. PCNA stains proliferating spermatogonia and later-stage spermatocytes that are not undergoing DNA synthesis [36]. Figure 5 shows positive staining of proliferating spermatocytes in

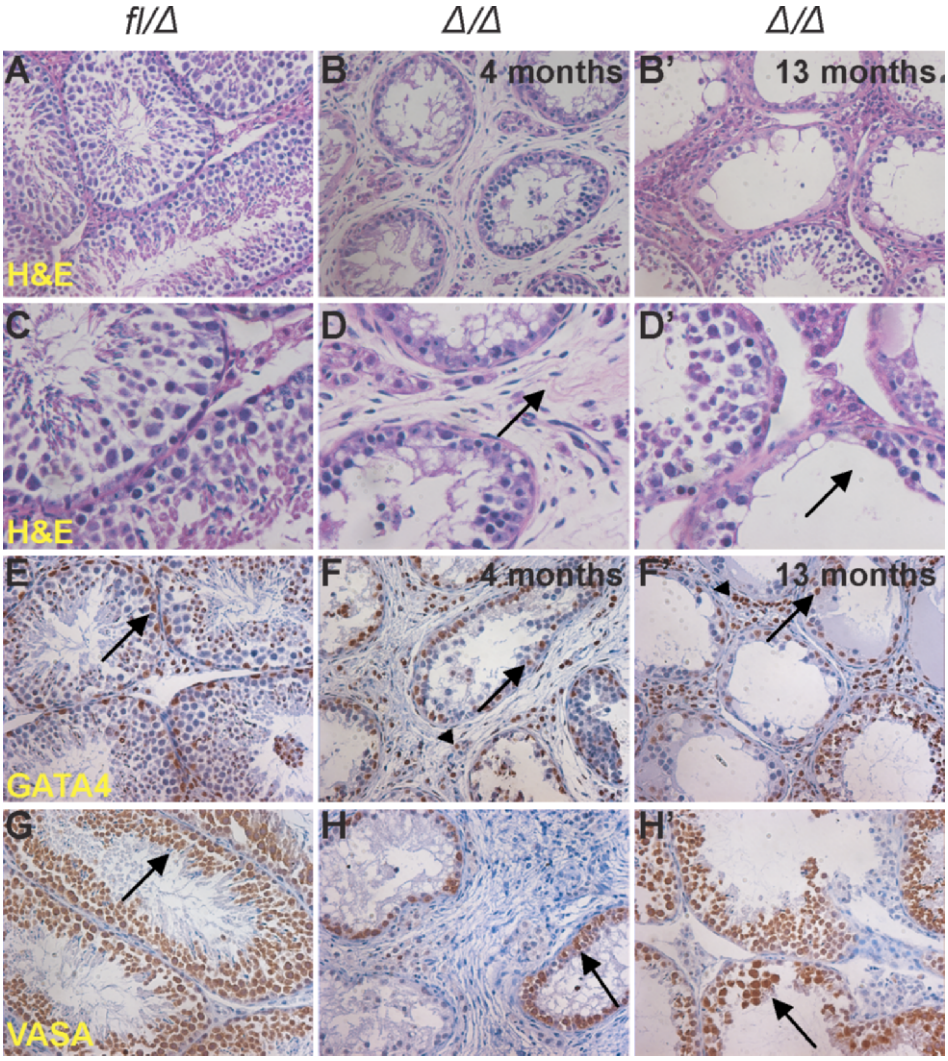

FIG. 6. The testicular phenotype progresses with age in *Epas1*$^{\Delta/\Delta}$ mice. **A**) Histological analyses of 4-mo-old and 13-mo-old testes obtained from multiple *Epas1*-deficient males compared with control *Epas1*$^{fl/\Delta}$ testes (**A** and **C**). The H&E staining depicted a phenotype worse than that observed at age 2 mo. *Epas1*$^{\Delta/\Delta}$ seminiferous tubules had lost increased numbers of germ cells, and the interstitial space was fibrotic (**B**, **B′**, **D**, and **D′** [arrows]). GATA4 and VASA expression was used to identify Sertoli cells (**E**–**F′** [arrows]) and germ cells (**G**–**H′** [arrows]); both were still present. GATA4 also detected Leydig cells in the interstitial space (**E**–**F′** [arrowheads]). Original magnification ×200 (**A**–**B′** and **E**–**H′**) and ×400 (**C**–**D′**).

control (Fig. 5A) and *Epas1*$^{\Delta/\Delta}$ (Fig. 5B) testes, and the number of proliferating cells per tubule cross-section was not decreased in *Epas1*$^{\Delta/\Delta}$ samples (n = 3–5). Apoptotic cells were occasionally detected in seminiferous tubules by cleaved caspase 3 staining in control and *Epas1*$^{\Delta/\Delta}$ testes, but no increase in *Epas1*$^{\Delta/\Delta}$ testes was apparent (Fig. 5, C and D). Because we failed to identify haploid cell types in *Epas1*$^{\Delta/\Delta}$ testes, we determined that *Epas1* deficiency inhibits spermatocytes to enter, proceed with, or exit meiosis. The histone variant H2AFX is phosphorylated in response to double-strand breaks occurring during crossovers between chromosomes in meiosis [37–39]. Strong staining of all metaphase chromosomes was detected in early spermatocytes, and phospho-H2AFX became restricted to the XY body as the cells proceeded through meiosis. Figure 5, E and F, shows a similar picture of phospho-H2AFX^{+} cells in control and *Epas1*$^{\Delta/\Delta}$ testes. In addition to H2AFX phosphorylation, we also analyzed meiotic cells by IF for synaptonemal complex protein-3 (SYCP3), which is important for binding the two sister chromatids during meiosis [40]. However, no defect was detected at this stage in *Epas1*$^{\Delta/\Delta}$ testes either (Fig. 5, G and H). Although multiple layers of postmeiotic germ cells visualized by 4′,6′-diamidino-2-phenylindole staining were present in control seminiferous tubules, a marked 40% reduction of haploid cells was observed in *Epas1*-deficient tubules. We performed RT-PCR analyses for calmegin (*Clgn*) and *Mybl1*, two genes expressed during meiosis, specifically in pachytene spermatocytes [41, 42]. Normal spermatocyte maturation was verified, as these genes were expressed normally in *Epas1*$^{\Delta/\Delta}$ testes. Glycerol 3-phosphate dehydrogenase (*Gpd*) was used as a loading control (Fig. 5, I–K).

In summary, we characterized the effect of postnatal *Epas1* ablation on germ cell differentiation and revealed loss of spermatids and spermatozoa in testes lacking EPAS1 activity. We found no evidence for a germ cell-intrinsic defect and therefore hypothesized that cell nonautonomous factors expressed by Sertoli cells in an EPAS1-dependent manner function in germ cell maturation. Spermatogenesis is controlled by many factors; these include hormones such as testosterone (secreted by Leydig cells) signaling to the androgen receptor on Sertoli cells. Given that Leydig cells also express EPAS1 [43], we measured testosterone levels in the serum of *Epas1*$^{\Delta/\Delta}$ males and their littermate controls (n = 5); however, testosterone levels were not altered in response to *Epas1* deficiency (Fig. 5L).

The Phenotype Observed in Epas1$^{\Delta/\Delta}$ *Testes Progresses with Age*

Analysis of testes from older males demonstrated that later in life (at ages 4, 7, and 13 mo) *Epas1*$^{\Delta/\Delta}$ testes lost additional germ cells and 50% of *Epas1*$^{\Delta/\Delta}$ animals showed signs of testicular fibrosis (n = 3–5) (Fig. 6, B, B′, D, and D′). We performed IHC for GATA4 and VASA to determine the nature of the few cells remaining in the seminiferous tubules of aged

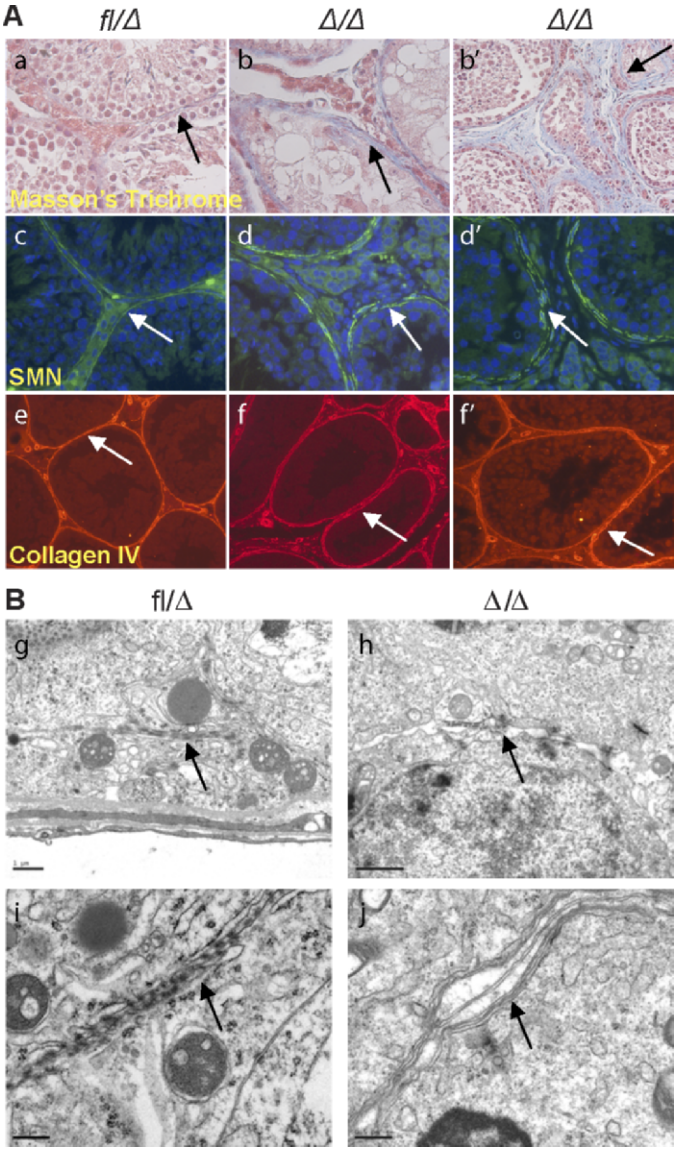

FIG. 7. *Epas*$^{\Delta/\Delta}$ testes exhibit defective basement membrane and myoid cell layers. **A**) Masson trichrome staining confirmed the fibroblastic character in the interstitial space of *Epas1*$^{\Delta/\Delta}$ mice (**a**, arrow) (original magnification ×400). *Epas1*$^{\Delta/\Delta}$ testes aged 4 mo (**b**) and 13 mo (**b′**) are shown. Myoid cells were detected by SMA IF (**c**); control seminiferous tubules were surrounded by a single layer of continuous myoid cells, promoting a tight basement membrane (arrow) (original magnification ×400). However, *Epas1*$^{\Delta/\Delta}$ testes displayed thickening and disruption of the basement membrane (**d** and **d′**, arrows) (original magnification ×400); the fibroblast-like cells in the interstitial space did not express SMN. Collagen type IV staining delineated irregularity and thickening of the basement membrane of mutant tubules (**e**–**f′**, arrows) (original magnification ×200). **B**) Electron microscopy displayed tight junctions and an impermeable seal between the membranes of two Sertoli cells in control testes (**g** and **i**, arrows). *Epas1*$^{\Delta/\Delta}$ testes contained shortened tight junctions (arrow in **h**) and did not form a proper barrier or seal (arrow in **j**). Furthermore, cells within *Epas1*$^{\Delta/\Delta}$ seminiferous tubules were surrounded by multiple membranes (arrow in **j**). Bar = 1 μm (**g**, **h**) and 0.5 μm (**i**, **j**).

Epas1$^{\Delta/\Delta}$ males. As described for 2-mo-old testes, GATA4^{+} Sertoli cells were located adjacent to the basement membrane in normal numbers. In addition to Sertoli cells, GATA4 immunoreactivity was also detected in Leydig cells in the interstitial space (Fig. 6, F and F′). Some *Epas1*$^{\Delta/\Delta}$ tubules were devoid of germ cells at this stage, whereas reduced numbers of germ cells were observed in others. The representation of tubules in different stages of the seminiferous cycle on cross-section through the testis could be a possible explanation for this variability (Fig. 6, H and H′). Masson trichrome staining allowed us to further analyze the fibrotic nature of the interstitial space in *Epas1*$^{\Delta/\Delta}$ samples. In control testes, only a thin layer of collagen forming the basement membrane exhibited blue staining (Fig. 7A, a). *Epas1*$^{\Delta/\Delta}$ testes, however, showed Masson trichrome positivity in the thin fibroblastic cells in the interstitial space, as well as a thickening of the basement membrane (Fig. 7A, b and b′). As shown in Figure 7A (b′), increased staining was observed in testes harvested from older animals.

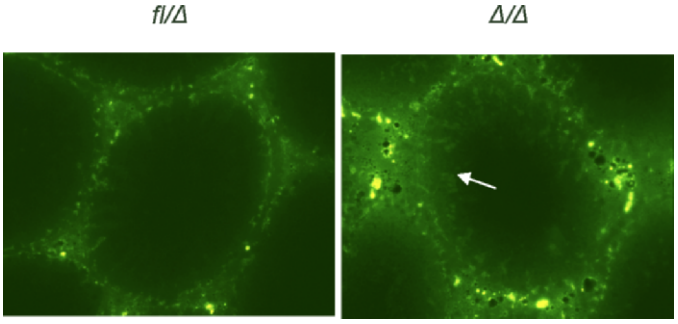

FIG. 8. Integrity of the BTB is impaired in *Epas1*$^{\Delta/\Delta}$ testes. The functional integrity assay displayed increased diffusion of FITC into the seminiferous tubules of *Epas1*$^{\Delta/\Delta}$ testes (arrow). In direct contrast, FITC staining is confined to the basal region of the seminiferous epithelium of control testes. Original magnification ×400.

Loss of Epas1 *Leads to Disruption of the Basement Membrane and BTB*

To evaluate the peritubular myoid cells in *Epas1*$^{\Delta/\Delta}$ testes, we performed IF for smooth muscle actin (SMA) expression [44] (Fig. 7A, c, d, and d′) in control and *Epas1*$^{\Delta/\Delta}$ testes (n = 3–5). The fibroblast-like cells in the interstitial space of *Epas1*$^{\Delta/\Delta}$ testes did not stain positive for SMA, indicating they were not derived from myoid cells. Instead of a single closed circle of myoid cells, *Epas1*$^{\Delta/\Delta}$ tubules were surrounded by several layers of myoid cells that failed to form a discrete barrier (Fig. 7A, d and d′). We also analyzed the expression of collagen type IV to evaluate the integrity of the basement membrane. Collagen type IV staining revealed an irregularity in the organization and a thickening (approximately 2-fold) of the basement membrane in *Epas1*$^{\Delta/\Delta}$ testes (Fig. 7A, e, f, and f′). Consistent with Masson trichrome staining, collagen type IV staining was also observed in the interstitial space. Importantly, a disrupted basement membrane could result in defective growth factor and endocrine signaling.

To pursue this observation, we investigated if *Epas1*$^{\Delta/\Delta}$ Sertoli cells established a functional BTB. The BTB is formed through Sertoli cell-Sertoli cell tight junctions separating spermatogonia from spermatocytes, spermatids, and spermatozoa to ensure normal maturation. Malfunctioning Sertoli cells, incapable of establishing the BTB or germ cell connections, would likely result in premature release of undifferentiated spermatocytes and spermatids. Electron microscopy (EM) was used to test this hypothesis. Sertoli cell-Sertoli cell tight junctions created a tight seal, forming the BTB in control testes (Fig. 7B, g and i). *Epas1*$^{\Delta/\Delta}$ Sertoli cells formed short stretches of tight junctions; however, a sealed barrier was not established (Fig. 7B, h and j). Furthermore, spaces between junctions formed by *Epas1*$^{\Delta/\Delta}$ Sertoli cells were visible, and cell membranes contained vesicles (Fig. 7B, j). Interestingly, *Epas1*$^{\Delta/\Delta}$ cells within the seminiferous tubules were surrounded by multiple membrane layers, and membranes appeared to

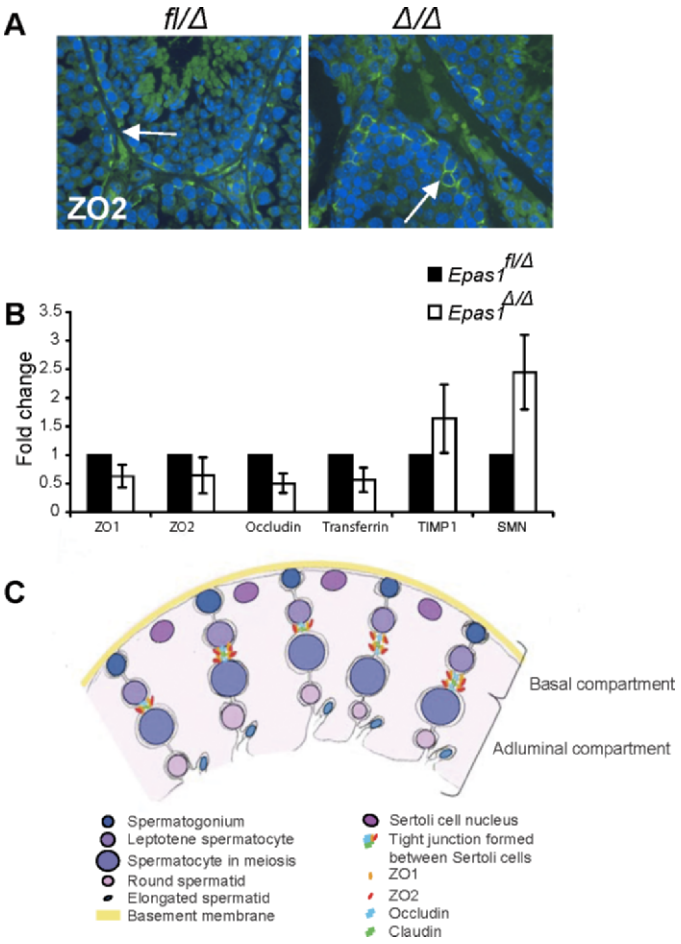

FIG. 9. Tight junction proteins are affected in *Epas1*$^{\Delta/\Delta}$ testes. **A**) ZO2 protein was still detected by IF in both control and *Epas1*$^{\Delta/\Delta}$ testes (arrows, original magnification ×400). **B**) The mRNAs encoding ZO1, ZO2, occludin, and transferrin were somewhat decreased in *Epas1*$^{\Delta/\Delta}$ testes. In contrast, the protease inhibitor TIMP1 and SMN (reflecting the myoid cell phenotype) were slightly increased in *Epas1*$^{\Delta/\Delta}$ mice (n = 4). Changes in relative abundance of these transcripts were not statistically significantly; however, all four mutant animals clearly displayed a trend toward decreased expression of each gene. **C**) Schematic drawing showing the different cell types, junctions, and compartments present in the seminiferous tubules. Sertoli cell nuclei (dark pink) are located close to the basement membrane (yellow), but their cytoplasm (light pink) reaches down to the lumen and connects with other Sertoli cells and germ cells. Tight junctions are formed between two Sertoli cells via ZO1, ZO2, occludin, and claudin interaction and divide the seminiferous tubule into a basal and adluminal compartment. Germ cells move toward the lumen as they mature. Spermatogonia (dark blue) are attached to the basement membrane. Once germ cells enter meiosis, they have passed the BTB and are now separated from blood and lymph. Mature spermatozoa are released into the lumen (light blue).

be significantly thicker (Fig. 7B, j). In addition to defects in Sertoli cell-Sertoli cell tight junctions, the connections formed between Sertoli cells and germ cells also appeared to be abnormal (data not shown).

To directly analyze the integrity of the BTB in *Epas1*$^{\Delta/\Delta}$ testes, we performed a functional assay that monitors the diffusion of a small fluorescent dye, FITC, across the BTB after administration via tail vein injection. Because the BTB is a selective barrier that prevents diffusion from the systemic circulation to the seminiferous epithelium [45], FITC was confined to the basal region of control tubules. However, in *Epas1*$^{\Delta/\Delta}$ testes, FITC was detected toward the middle of tubule lumens, suggesting damage to BTB integrity (Fig. 8). Several junction proteins (such as members of the zona occludens family [ZO1, ZO2, and occludin], as well as claudins) are essential for functional tight junctions and spermatogenesis [46–48]. We performed IF staining for several of these junction proteins and detected the presence of ZO1, ZO2, and occludin in discrete spots between cells located at the basement membrane (Fig. 9A and data not shown). In agreement with EM analyses, loss of *Epas1* did not completely ablate the expression of tight junction proteins. It is, however, possible that the tight junctions detected are not functional or present in normal numbers.

Because IF is not a reliable tool for protein quantification, we performed quantitative RT-PCR for ZO1, ZO2, and occludin on whole-testis RNA. We compared each *Epas1*$^{\Delta/\Delta}$ animal with a littermate control and averaged the fold changes observed from four *Epas1*$^{\Delta/\Delta}$-*Epas1*$^{fl/\Delta}$ pairs. We detected a 25%–50% reduction in mRNA levels of the tight junction components ZO1, ZO2, and occludin (Fig. 9B). Another Sertoli cell gene product important for regulating spermatogenesis is transferrin, a protein having a critical role in shuttling iron from Sertoli cells to germ cells [49]. Transferrin has been suggested to be a HIF target gene [50, 51], and transferrin mRNA levels were somewhat reduced in *Epas1*$^{\Delta/\Delta}$ testes (Fig. 9B). This is intriguing because decreased transferrin levels should also contribute to disrupted spermatogenesis in *Epas1*$^{\Delta/\Delta}$ animals. The third class of glycoproteins expressed by Sertoli cells includes proteases and protease inhibitors. We did not detect dramatic changes in matrix metalloprotease *Mmp2* or *Mmp3* mRNA levels (data not shown) but found that mRNA levels of the protease inhibitor *Timp1* were slightly increased (Fig. 9B). The changes in these mRNA transcripts were not statistically significant between the *Epas1*$^{\Delta/\Delta}$-*Epas1*$^{fl/\Delta}$ pairs, but a trend was clearly observed at the gene expression level. Altogether, we demonstrate that postnatal depletion of EPAS1 in the testis affects the structural components of the basement membrane and Sertoli cell tight junction complexes, resulting in defective BTB and thereby affecting the retention of spermatids.

DISCUSSION

Epas1 expression is restricted to distinct cell populations in the brain, heart, lung, kidney, liver, pancreas, and intestine, whereas HIF-1α is ubiquitously expressed [23, 43, 52]. EPAS1 is essential for development, as global *Epas1* deletion causes embryonic and/or perinatal lethality [18, 21, 23]. We have previously reported that acute postnatal deletion of *Epas1* results in anemia [25]. To understand the role of this important transcription factor during spermatogenesis, we deleted *Epas1* 2.5 days after birth via a ubiquitously expressed inducible Cre transgene (UBC-Cre) and analyzed the testes of control and *Epas1*$^{\Delta/\Delta}$ males after the animals completed puberty. *Epas1* deficiency resulted in infertility due to substantially reduced sperm counts. This manifested itself through a reduction in testis size and weight. Several explanations for this defect have been investigated. Defective spermatogenesis can be due to failure to maintain the SSC pool [53, 54], increased apoptosis in response to meiotic arrest, and/or ineffective proliferation or premature release of germ cells. Loss of stem cell maintenance genes, RNA-binding proteins, and Piwi-interacting RNA processing factors [55, 56] and ineffective hormonal and growth factor signaling [57, 58] result in maturation defects and oligospermia or azoospermia [59]. Such phenotypes can be caused by germ cell-intrinsic defects and by mutations in supporting cells [60, 61].

Analysis of *Epas1*$^{\Delta/\Delta}$ testis morphology established a gradual loss of germ cells, specifically spermatids. Sertoli cell number and localization were unchanged, despite Sertoli cell-

restricted EPAS1 expression within testicular tubules. POU5F1$^+$ spermatogonia, as well as meiotic spermatocytes expressing SYCP3 (SCP-3), MYBL1 (A-myb), Calmegin, and H2AFX (γ-H2AX), were present in 2-mo-old *Epas1*$^{\Delta/\Delta}$ testes. Haploid FE-J1$^+$spermatids, however, were largely missing. Furthermore, VASA$^+$ germ cell numbers were reduced at age 2 mo and decreased further with age. For unexplained reasons, the interstitial space of *Epas1*$^{\Delta/\Delta}$ testes was filled with fibroblast-like cells first detected at age 4 mo. Serum testosterone levels were not altered as a result of *Epas1* deletion. Because increasing numbers of immature germ cells were lost with age, we concluded that this phenotype was not the consequence of a maturation defect arresting germ cells at a specific differentiation stage. In contrast, the data suggest malfunctioning Sertoli cells and/or peritubular myoid cells surrounding the basement membrane, leading to loss of germ cells as a result of ineffective binding to cells within the seminiferous tubules. Of note, some round spermatids could be detected in the epididymis of *Epas1*$^{\Delta/\Delta}$ animals, indicating they are being shed from these structures.

Sertoli cell-Sertoli cell tight junctions and adherence junctions establish a flexible mechanism capable of opening and closing to allow germ cells to move from the basement membrane to the lumen as they progress in the seminiferous cycle [62]. *Epas1*$^{\Delta/\Delta}$ testes did not form normal tight junctions, and it appears that EPAS1 regulates the expression of junction proteins such as claudins and members of the zona occludins family. This is supported by our quantitative RT-PCR data that suggest a decrease in the expression of multiple tight junction protein genes and EM images that indicate fewer junctions. Premature release of germ cells could be caused by breakdown of the basement membrane, as well as by failure of Sertoli cells to effectively connect to germ cells and hold them inside the testicular tubules. In a different biological system, specific deletion of *Epas1* in mouse ECs increased vessel permeability and caused aberrant EC ultrastructure [63]. Moreover, immortalized *Epas1*-deficient ECs displayed reduced adhesion to extracellular matrix proteins [63], implicating the importance of EPAS1 in maintenance of the integrity of membranous structures.

The importance of a specific microenvironment in regulating tissue homeostasis has been described for a number of organs. Germ cells and somatic Sertoli cells are enclosed in the seminiferous tubules, which develop from the sex cords. The SSCs are scattered throughout the length of the seminiferous tubules, which form loops and are tightly packed within the tunica albuginea, the outer capsule of the testis. The interstitial space between the seminiferous tubules is filled with Leydig cells, blood vessels, and macrophages. Leydig cells also contribute to the spermatogonial microenvironment by secreting growth factors and hormones [64]. A recent study by Yoshida et al. [65] describes the importance of blood vessels in providing a possible niche for SSCs. This group showed in a series of elegant experiments that A_{undiff} spermatogonia primarily reside close to blood vessels, accompanied by interstitial cells, especially at vascular branches. Once the cells differentiate, they move farther away from vessels, and differentiated spermatogonia, spermatocytes, and spermatids are found in the lumen.

Hypoxia in general and HIFs in particular markedly contribute to providing signals for proliferation and differentiation. The present study presents a novel role for EPAS1 in regulating spermatogenesis. While *Epas1* deficiency did not eliminate the expression of a single junction protein, decreased expression of multiple proteins should decrease the ability to form a fully functional BTB. This could lead to loss of germ cells due to improper contact and junction formation. EPAS1 is also likely to be involved in regulating basement membrane integrity via an interaction between Sertoli cells and peritubular myoid cells. Additional studies will increase our understanding of the important roles of Sertoli cells, the basement membrane, and O_2 levels during spermatogenesis.

ACKNOWLEDGMENTS

We thank Jennifer Lam, Hongwei Yu, and Q.C. Yu, members of the Simon laboratory, for technical assistance and Drs. George Gerton, Norman Hecht, James Kehler, Steve Dinardo, Haifan Lin, and Jeremy Wang for helpful discussions and advice.

REFERENCES

1. Vergouwen RP, Huiskamp R, Bas RJ, Roepers-Gajadien HL, Davids JA, de Rooij DG. Postnatal development of testicular cell populations in mice. J Reprod Fertil 1993; 99:479–485.
2. Dym M, Fawcett DW. The blood-testis barrier in the rat and the physiological compartmentation of the seminiferous epithelium. Biol Reprod 1970; 3:308–326.
3. Griswold MD. Interactions between germ cells and Sertoli cells in the testis. Biol Reprod 1995; 52:211–216.
4. Russell LD, Peterson RN. Sertoli cell junctions: morphological and functional correlates. Int Rev Cytol 1985; 94:177–211.
5. Wenger RH, Katschinski DM. The hypoxic testis and post-meiotic expression of PAS domain proteins. Semin Cell Dev Biol 2005; 16:547–553.
6. Giaccia AJ, Simon MC, Johnson R. The biology of hypoxia: the role of oxygen sensing in development, normal function, and disease. Genes Dev 2004; 18:2183–2194.
7. Schofield CJ, Ratcliffe PJ. Oxygen sensing by HIF hydroxylases. Nat Rev Mol Cell Biol 2004; 5:343–354.
8. Semenza GL. HIF-1 and mechanisms of hypoxia sensing. Curr Opin Cell Biol 2001; 13:167–171.
9. Ivan M, Kondo K, Yang H, Kim W, Valiando J, Ohh M, Salic A, Asara JM, Lane WS, Kaelin WG Jr. HIFalpha targeted for VHL-mediated destruction by proline hydroxylation: implications for O_2 sensing. Science 2001; 292:464–468.
10. Jaakkola P, Mole DR, Tian YM, Wilson MI, Gielbert J, Gaskell SJ, Kriegsheim A, Hebestreit HF, Mukherji M, Schofield CJ, Maxwell PH, Pugh CW, et al. Targeting of HIF-alpha to the von Hippel-Lindau ubiquitylation complex by O_2-regulated prolyl hydroxylation. Science 2001; 292:468–472.
11. Yu F, White SB, Zhao Q, Lee FS. HIF-1alpha binding to VHL is regulated by stimulus-sensitive proline hydroxylation. Proc Natl Acad Sci U S A 2001; 98:9630–9635.
12. Patel SA, Simon MC. Biology of hypoxia-inducible factor-2alpha in development and disease. Cell Death Differ 2008; 15:628–634.
13. Hu CJ, Wang LY, Chodosh LA, Keith B, Simon MC. Differential roles of hypoxia-inducible factor 1alpha (HIF-1alpha) and HIF-2alpha in hypoxic gene regulation. Mol Cell Biol 2003; 23:9361–9374.
14. Depping R, Hagele S, Wagner KF, Wiesner RJ, Camenisch G, Wenger RH, Katschinski DM. A dominant-negative isoform of hypoxia-inducible factor-1 alpha specifically expressed in human testis. Biol Reprod 2004; 71:331–339.
15. Powell JD, Elshtein R, Forest DJ, Palladino MA. Stimulation of hypoxia-inducible factor-1 alpha (HIF-1alpha) protein in the adult rat testis following ischemic injury occurs without an increase in HIF-1alpha messenger RNA expression. Biol Reprod 2002; 67:995–1002.
16. Lysiak JJ, Kirby JL, Tremblay JJ, Woodson RI, Reardon MA, Palmer LA, Turner TT. Hypoxia-inducible factor-1alpha is constitutively expressed in murine Leydig cells and regulates 3beta-hydroxysteroid dehydrogenase type 1 promoter activity. J Androl 2009; 30:146–156.
17. Marti HH, Katschinski DM, Wagner KF, Schaffer L, Stier B, Wenger RH. Isoform-specific expression of hypoxia-inducible factor-1alpha during the late stages of mouse spermiogenesis. Mol Endocrinol 2002; 16:234–243.
18. Compernolle V, Brusselmans K, Acker T, Hoet P, Tjwa M, Beck H, Plaisance S, Dor Y, Keshet E, Lupu F, Nemery B, Dewerchin M, et al. Loss of HIF-2alpha and inhibition of VEGF impair fetal lung maturation, whereas treatment with VEGF prevents fatal respiratory distress in premature mice. Nat Med 2002; 8:702–710.
19. Iyer NV, Kotch LE, Agani F, Leung SW, Laughner E, Wenger RH, Gassmann M, Gearhart JD, Lawler AM, Yu AY, Semenza GL. Cellular and developmental control of O_2 homeostasis by hypoxia-inducible factor 1 alpha. Genes Dev 1998; 12:149–162.

20. Maltepe E, Schmidt JV, Baunoch D, Bradfield CA, Simon MC. Abnormal angiogenesis and responses to glucose and oxygen deprivation in mice lacking the protein ARNT. Nature 1997; 386:403–407.
21. Peng J, Zhang L, Drysdale L, Fong GH. The transcription factor EPAS-1/hypoxia-inducible factor 2alpha plays an important role in vascular remodeling. Proc Natl Acad Sci U S A 2000; 97:8386–8391.
22. Ryan HE, Lo J, Johnson RS. HIF-1 alpha is required for solid tumor formation and embryonic vascularization. EMBO J 1998; 17:3005–3015.
23. Tian H, Hammer RE, Matsumoto AM, Russell DW, McKnight SL. The hypoxia-responsive transcription factor EPAS1 is essential for catecholamine homeostasis and protection against heart failure during embryonic development. Genes Dev 1998; 12:3320–3324.
24. Cramer T, Yamanishi Y, Clausen BE, Forster I, Pawlinski R, Mackman N, Haase VH, Jaenisch R, Corr M, Nizet V, Firestein GS, Gerber HP, et al. HIF-1alpha is essential for myeloid cell-mediated inflammation. Cell 2003; 112:645–657.
25. Gruber M, Hu CJ, Johnson RS, Brown EJ, Keith B, Simon MC. Acute postnatal ablation of Hif-2alpha results in anemia. Proc Natl Acad Sci U S A 2007; 104:2301–2306.
26. Schipani E, Ryan HE, Didrickson S, Kobayashi T, Knight M, Johnson RS. Hypoxia in cartilage: HIF-1alpha is essential for chondrocyte growth arrest and survival. Genes Dev 2001; 15:2865–2876.
27. Seagroves TN, Ryan HE, Lu H, Wouters BG, Knapp M, Thibault P, Laderoute K, Johnson RS. Transcription factor HIF-1 is a necessary mediator of the Pasteur effect in mammalian cells. Mol Cell Biol 2001; 21:3436–3444.
28. Tomita S, Sinal CJ, Yim SH, Gonzalez FJ. Conditional disruption of the aryl hydrocarbon receptor nuclear translocator (Arnt) gene leads to loss of target gene induction by the aryl hydrocarbon receptor and hypoxia-inducible factor 1alpha. Mol Endocrinol 2000; 14:1674–1681.
29. Ruzankina Y, Pinzon-Guzman C, Asare A, Ong T, Pontano L, Cotsarelis G, Zediak VP, Velez M, Bhandoola A, Brown EJ. Deletion of the developmentally essential gene ATR in adult mice leads to age-related phenotypes and stem cell loss. Cell Stem Cell 2007; 1:113–126.
30. Tanaka SS, Toyooka Y, Akasu R, Katoh-Fukui Y, Nakahara Y, Suzuki R, Yokoyama M, Noce T. The mouse homolog of Drosophila Vasa is required for the development of male germ cells. Genes Dev 2000; 14:841–853.
31. Ryan HE, Poloni M, McNulty W, Elson D, Gassmann M, Arbeit JM, Johnson RS. Hypoxia-inducible factor-1alpha is a positive factor in solid tumor growth. Cancer Res 2000; 60:4010–4015.
32. Raleigh JA, Chou SC, Tables L, Suchindran S, Varia MA, Horsman MR. Relationship of hypoxia to metallothionein expression in murine tumors. Int J Radiat Oncol Biol Phys 1998; 42:727–730.
33. Ketola I, Rahman N, Toppari J, Bielinska M, Porter-Tinge SB, Tapanainen JS, Huhtaniemi IT, Wilson DB, Heikinheimo M. Expression and regulation of transcription factors GATA-4 and GATA-6 in developing mouse testis. Endocrinology 1999; 140:1470–1480.
34. Kehler J, Tolkunova E, Koschorz B, Pesce M, Gentile L, Boiani M, Lomeli H, Nagy A, McLaughlin KJ, Scholer HR, Tomilin A. Oct4 is required for primordial germ cell survival. EMBO Rep 2004; 5:1078–1083.
35. Fenderson BA, O'Brien DA, Millette CF, Eddy EM. Stage-specific expression of three cell surface carbohydrate antigens during murine spermatogenesis detected with monoclonal antibodies. Dev Biol 1984; 103:117–128.
36. Chapman DL, Wolgemuth DJ. Expression of proliferating cell nuclear antigen in the mouse germ line and surrounding somatic cells suggests both proliferation-dependent and -independent modes of function. Int J Dev Biol 1994; 38:491–497.
37. Celeste A, Petersen S, Romanienko PJ, Fernandez-Capetillo O, Chen HT, Sedelnikova OA, Reina-San-Martin B, Coppola V, Meffre E, Difilippantonio MJ, Redon C, Pilch DR, et al. Genomic instability in mice lacking histone H2AX. Science 2002; 296:922–927.
38. Fernandez-Capetillo O, Mahadevaiah SK, Celeste A, Romanienko PJ, Camerini-Otero RD, Bonner WM, Manova K, Burgoyne P, Nussenzweig A. H2AX is required for chromatin remodeling and inactivation of sex chromosomes in male mouse meiosis. Dev Cell 2003; 4:497–508.
39. Hamer G, Roepers-Gajadien HL, van Duyn-Goedhart A, Gademan IS, Kal HB, van Buul PP, de Rooij DG. DNA double-strand breaks and gamma-H2AX signaling in the testis. Biol Reprod 2003; 68:628–634.
40. Yuan L, Liu JG, Zhao J, Brundell E, Daneholt B, Hoog C. The murine SCP3 gene is required for synaptonemal complex assembly, chromosome synapsis, and male fertility. Mol Cell 2000; 5:73–83.
41. Mettus RV, Litvin J, Wali A, Toscani A, Latham K, Hatton K, Reddy EP. Murine A-myb: evidence for differential splicing and tissue-specific expression. Oncogene 1994; 9:3077–3086.
42. Watanabe D, Yamada K, Nishina Y, Tajima Y, Koshimizu U, Nagata A, Nishimune Y. Molecular cloning of a novel Ca(2+)-binding protein (calmegin) specifically expressed during male meiotic germ cell development. J Biol Chem 1994; 269:7744–7749.
43. Jain S, Maltepe E, Lu MM, Simon C, Bradfield CA. Expression of ARNT, ARNT2, HIF1 alpha, HIF2 alpha and Ah receptor mRNAs in the developing mouse. Mech Dev 1998; 73:117–123.
44. Tung PS, Fritz IB. Characterization of rat testicular peritubular myoid cells in culture: alpha-smooth muscle isoactin is a specific differentiation marker. Biol Reprod 1990; 42:351–365.
45. Xia W, Mruk DD, Cheng CY. C-type natriuretic peptide regulates blood-testis barrier dynamics in adult rat testes. Proc Natl Acad Sci U S A 2007; 104:3841–3846.
46. Fanning AS, Mitic LL, Anderson JM. Transmembrane proteins in the tight junction barrier. J Am Soc Nephrol 1999; 10:1337–1345.
47. Furuse M, Hirase T, Itoh M, Nagafuchi A, Yonemura S, Tsukita S, Tsukita S. Occludin: a novel integral membrane protein localizing at tight junctions. J Cell Biol 1993; 123:1777–1788.
48. Lui WY, Mruk D, Lee WM, Cheng CY. Sertoli cell tight junction dynamics: their regulation during spermatogenesis. Biol Reprod 2003; 68:1087–1097.
49. Sylvester SR, Griswold MD. The testicular iron shuttle: a ''nurse'' function of the Sertoli cells. J Androl 1994; 15:381–385.
50. Lok CN, Ponka P. Identification of a hypoxia response element in the transferrin receptor gene. J Biol Chem 1999; 274:24147–24152.
51. Rolfs A, Kvietikova I, Gassmann M, Wenger RH. Oxygen-regulated transferrin expression is mediated by hypoxia-inducible factor-1. J Biol Chem 1997; 272:20055–20062.
52. Wiesener MS, Jurgensen JS, Rosenberger C, Scholze CK, Horstrup JH, Warnecke C, Mandriota S, Bechmann I, Frei UA, Pugh CW, Ratcliffe PJ, Bachmann S, et al. Widespread hypoxia-inducible expression of HIF-2alpha in distinct cell populations of different organs. FASEB J 2003; 17:271–273.
53. Buaas FW, Kirsh AL, Sharma M, McLean DJ, Morris JL, Griswold MD, de Rooij DG, Braun RE. Plzf is required in adult male germ cells for stem cell self-renewal. Nat Genet 2004; 36:647–652.
54. Costoya JA, Hobbs RM, Barna M, Cattoretti G, Manova K, Sukhwani M, Orwig KE, Wolgemuth DJ, Pandolfi PP. Essential role of Plzf in maintenance of spermatogonial stem cells. Nat Genet 2004; 36:653–659.
55. Carmell MA, Girard A, van de Kant HJ, Bourc'his D, Bestor TH, de Rooij DG, Hannon GJ. MIWI2 is essential for spermatogenesis and repression of transposons in the mouse male germline. Dev Cell 2007; 12:503–514.
56. Kuramochi-Miyagawa S, Kimura T, Ijiri TW, Isobe T, Asada N, Fujita Y, Ikawa M, Iwai N, Okabe M, Deng W, Lin H, Matsuda Y, et al. Mili, a mammalian member of piwi family gene, is essential for spermatogenesis. Development 2004; 131:839–849.
57. Chen C, Ouyang W, Grigura V, Zhou Q, Carnes K, Lim H, Zhao GQ, Arber S, Kurpios N, Murphy TL, Cheng AM, Hassell JA, et al. ERM is required for transcriptional control of the spermatogonial stem cell niche. Nature 2005; 436:1030–1034.
58. Naughton CK, Jain S, Strickland AM, Gupta A, Milbrandt J. Glial cell-line derived neurotrophic factor-mediated RET signaling regulates spermatogonial stem cell fate. Biol Reprod 2006; 74:314–321.
59. Behr R, Sackett SD, Bochkis IM, Le PP, Kaestner KH. Impaired male fertility and atrophy of seminiferous tubules caused by haploinsufficiency for Foxa3. Dev Biol 2007; 306:636–645.
60. De Gendt K, Swinnen JV, Saunders PT, Schoonjans L, Dewerchin M, Devos A, Tan K, Atanassova N, Claessens F, Lecureuil C, Heyns W, Carmeliet P, et al. A Sertoli cell-selective knockout of the androgen receptor causes spermatogenic arrest in meiosis. Proc Natl Acad Sci U S A 2004; 101:1327–1332.
61. Ryu BY, Orwig KE, Oatley JM, Avarbock MR, Brinster RL. Effects of aging and niche microenvironment on spermatogonial stem cell self-renewal. Stem Cells 2006; 24:1505–1511.
62. Mruk DD, Cheng CY. Sertoli-Sertoli and Sertoli-germ cell interactions and their significance in germ cell movement in the seminiferous epithelium during spermatogenesis. Endocr Rev 2004; 25:747–806.
63. Skuli N, Liu L, Runge A, Wang T, Yuan L, Patel S, Iruela-Arispe L, Simon MC, Keith B. Endothelial deletion of hypoxia-inducible factor-2alpha (HIF-2alpha) alters vascular function and tumor angiogenesis. Blood 2009; 114:469–477.
64. Holdcraft RW, Braun RE. Hormonal regulation of spermatogenesis. Int J Androl 2004; 27:335–342.
65. Yoshida S, Sukeno M, Nabeshima Y. A vasculature-associated niche for undifferentiated spermatogonia in the mouse testis. Science 2007; 317:1722–1726.